UNIVERSITY OF CRETE

MASTER THESIS

Entropy and Quantum Information in the Biochemical Reactions of the Magnetic Compass

---

Author:
Kostas Mouloudakis

Supervisor:
Prof. Iannis Kominis

A thesis submitted in fulfilment of the requirements
for the degree of Masters of Science in the
Faculty of Physics

ΠΑΝΕΠΙΣΤΗΜΙΟ
ΚΡΗΤΗΣ

UNIVERSITY
OF CRETE

September 17, 2016

UNIVERSITY OF CRETE

Abstract

Department of Physics

Entropy and Quantum Information in the Biochemical Reactions of the Magnetic Compass

Radical-ion-pair reactions, central for understanding the avian magnetic compass and spin transport in photosynthetic reaction centers, were recently shown to be a fruitful paradigm of the new synthesis of quantum information science with biological processes. We here show that the master equation so far constituting the theoretical foundation of spin chemistry violates fundamental bounds for the entropy of quantum systems. In contrast, a new theory based on quantum measurements, quantum coherence measures and quantum retrodiction, thus exemplifying the paradigm of quantum biology, satisfies the same bounds. By considering the quantum information extracted during the reaction we also unravel new magnetic-field effects not conveyed by reaction yields. The results of the thesis are uploaded in $arXiv: 1607.03071$

Acknowledgements

First of all, I would like to thank my supervisor Iannis Kominis for all the guidance and support that he offered me, for the great collaboration we have and for the continuous transfer of knowledge he provide us. I would also like to thank my brother George Mouloudakis for all the enlightening discussions we have. Furthermore, I would like to mention professors Peter Lambropoulos, Peter Rakitzis and Wolf von Klitzing for their guidance, assistance and support and last but not least, I would love to thank my family, my friends and colleagues Komis Giannis, Manolis Petrakakis, Sophie Tsiatsiou, Xristos Panagiotou, Vitalis Kuriakos, Saliaris Kostas and all the other members of our group.

Contents

Abstract **iii**

Acknowledgements **v**

1 Introduction **1**
1.1 Quantum Biology 1
1.2 Quantum Information and the Radical-Pair Dynamics 1
1.3 In This Thesis 2

2 Master Equation Description of the Radical-Pair Mechanism **5**
2.1 Brief Review of the Radical-Pair Mechanism 5
2.2 The Hamiltonian 7
2.3 Master Equations 8
2.3.1 Haberkorn's Master Equation 9
2.3.2 Kominis' Master Equation 10

3 Entropy of Quantum Systems: The Radical-Pair System **13**
3.1 Quantum Measurement and Entropy 13
3.2 The Spin-1 Paradigm 16
3.3 Ozawa Entropy bound and the Radical-Pair Mechanism . . 17
3.3.1 Haberkorn's Master Equation Violates the Ozawa Entropy Bound 17
3.4 Conclusions-Discussion 24

List of Figures

2.1 Radical-Pair Reaction Cycle 6
2.2 Hamiltonian evolution 9
2.3 Singlet-Triplet Mixing 10
2.4 Radical-Pair Kominis Reaction Cycle 11

3.1 Spin-1 system: Ozawa Bound 17
3.2 Ozawa and Lanford-Robinson Bounds 19
3.3 New Field Effect 20
3.4 Singlet-Triplet Energies 22
3.5 Eigenstates as a Function of the Magnetic Field 22
3.6 Magnitude Field Effect 23
3.7 Angle Field Effect 23

Chapter 1

Introduction

1.1 Quantum Biology

A new synthesis of two emerging fields, physics and biology have been developed over the last several decades under the name of quantum biology, to give rise and insight into the light-dependent chemical reactions taking place in complex biological systems. This new synthesis tries to take advantage of phenomena like quantum entanglement, quantum coherence and decoherence, quantum measurements, quantum retrodiction and other quantum-information type effects in order to describe biological processes like light harvesting in photosynthesic reaction centers, avian compass magnetoreception, the mechanism of olfaction and the energy trasport in photosynthesis. By definition biological systems are open systems.They are embeddedin environment that are noisy warm and wet and there is a challenging question of how quantum coherence can survive in such environments. Recent studies have shown that quantum coherence and entanglement can not only survive but it can also be enhanced by the interaction between the system and the environment.

Although the field contains promisingly quantum effects, the fundamental master equation describing the chemical reaction processes is still an open question. In this thesis we use quantum information theory and quantum measurement theory in order to, first of all, provide a test to the two master equations based on some fundamental information bounds that must be satisfied by every physical system and last but not least to show that the Haberkorn's master equation violates some fundamental entropy bounds based on informational characteristics. Furthermore, we show that a modern master equation that Kominis derived through the years (2008-2014) satisfies the same bounds. Besides the test on the two theories, the quantum informational approach led to the observation of a new magnetic field effect that is not observed in the reaction's neutral yields and it is possibly an effect based on quantum coherence.

1.2 Quantum Information and the Radical-Pair Dynamics

Quantum dynamics seem to have an important role in Bio-molecular processes. Spin dynamics of such processes are of great importance since they underlie all the quantum effects that are crucial for understanding magneto-based processes such as the mechanism of migratory bird navigation, the dynamics of photosynthetic reaction centers and so on. The basic mechanism that describes such processes is the Radical Pair mechanism.The mechanism first introduced in 1960 in order to explain anomalously large EPR and NMR signals. Radical-pairs are molecular neighbour-pairs which are created by an optical excitation and a charge transfer. Our interest is concentrated at the spin dynamics of such pairs. When the charge transfer is completed, the (charge-polarized) radical-pair is created in an initial spin state (which for all practical purposes is pre-determined by the total angular momentum conservation) and evolves under the influence of local and global magnetic environments. At some point the charge transfer reverse process neutralizes the radical-pair spontaneously in a spin-dependent way and the "chemical reaction" is terminated in the sense that Hamiltonian evolution is not possible since the radical pair does not exist. Of course one could argue that a semi-classical description of such processes using rate equations and population transfer would describe fair enough the Bio-processes of interest (as usually done in Biology and Chemistry) but if coherent phenomena are slow enough (compared to system timescales) they can have a significant role in the evolution of the radical pair . This is the point where quantum coherence dynamics and quantum information merge together to create the quantum biology science.

There are many evidences that under certain conditions, coherence time scales in such environments are large enough compared to dissipation and relaxation times, thus a fully quantum description is needed and the best way to do so in such complex systems is by using a master equation description for the evolution of a well defined density matrix. Of course the measurement observables and the experimental outcomes are given by the expectation values of quantities that also a semi-classical theory would provide but in a high-decoherence way. Furthermore, with the development of theoretical quantum metrology, using a well-defined theory would lead to a greater insight at the rates of the system and the internal structure and would also lead to technological advances in high precision measurements. Besides quantum metrology, another modern and useful tool of quantum theory is the science of quantum information. Quantum information and branches of quantum information such as quantum communication, quantum retrodiction and quantum cryptography can provide powerful tools on establishing the fundamental theory of spin-dependent biological processes and on manipulating quantum coherence in a path of advanced technology which probably would lead to high-efficiency quantum computers and would open the road of quantum physics in biotechnology.

1.3 In This Thesis

This thesis is a great paradigm of the application of quantum information in the science of quantum biology. We apply the Ozawa and Lanford-Robinson entropy-information bounds in the fundamental theories of radical-pair spin dynamical processes. In more detail, we show that Haberkorn's master equation violates the above bounds in the case where $k_S \neq k_T$ while Kominis master equation is valid in all the parameter regimes. In chapter 2 we will review the radical-pair mechanism and the two competing theories in detail, while in chapter 3 we will present the entropy bounds and the response of the two theories to the fundamental inequalities. Finally we will discuss the new field effect that appeared.

Chapter 2

Master Equation Description of the Radical-Pair Mechanism

2.1 Brief Review of the Radical-Pair Mechanism

As mentioned in Chapter 1, quantum biology[1-3] has been recently emerging as an interdisciplinary field pointing to certain biological processes which, counterintuitively, exhibit quantum coherent dynamics, and accordingly require for their understanding physical concepts developed in quantum information science. This is surprising since decoherence is ordinary expected to be prevalent in complex biological matter. Yet, there appear to be several cases where decoherence is not as detrimental, and moreover, where quantum coherent dynamics seem to have an operational significance.

Prominent among such examples have been the excitation energy transport in photosynthetic light harvesting[4-9] and the radical-pair mechanism [3,10-18], which was introduced in the late 1960's [22] to explain unexpectedly large signals in NMR measurements of organic radicals. The mechanism is the cornerstone of spin chemistry and photochemistry studying the effects of electron and nuclear spins in chemical reactions [23]. Radical-pair reactions have been studied extensively because, besides their potential role in avian magnetoreception [19-21], they regulate spin transport in photosynthetic reaction centers [22].

The radical-pair mechanism has recently attracted renewed attention when it was suggested [10] that radical-pair reactions involve quantum measurement dynamics and require for their understanding concepts like quantum coherence measures and the quantum communications concept of quantum retrodiction [11,12], rendering the mechanism a vivid paradigm for quantum biology on the qualitative level. On the quantitative level, we have developed a master new equation describing the fundamental quantum dynamics of RP reactions [3], which depart from the traditional theory, attributed to Haberkorn [24]. The master equation describing the time evolution of the radical-pair spin density matrix is the starting point for virtually all theoretical predictions relevant to the radical-pair mechanism. Radical-ion pairs are biomolecular ions (each carrying an unpaired electron •) created by an electron transfer from a photo-excited donor-acceptor molecular dyad: $DA{\to}^{hv}D^{*}A \to D^{\bullet+}A^{\bullet-}$. The magnetic nuclei of D and A couple to the respective unpaired electron via hyperfine interactions, leading to singlet-triplet (S-T) mixing, i.e. a coherent oscillation of the spin state of the electrons and concomitantly the nuclear spins: ${}^{S}D^{\bullet+}A^{\bullet-}{\leftrightarrow}{}^{T}D^{\bullet+}A^{\bullet-}$. The reverse charge transfer, called charge recombination, terminates the reaction and spin-selectively leads to the formation of either singlet or triplet neutral reaction products. The theoretical description of radical-pair reactions is accounted for by the density matrix ρ describing the spin state of the molecule's two electrons and any number of present magnetic nuclei. In this work we will consider an radical-ion pair having just one nuclear spin-1/2 particle, hence the density matrix is 8-dimensional. A simplified schematic plot of energy levels of the reaction, is given in the following figure.

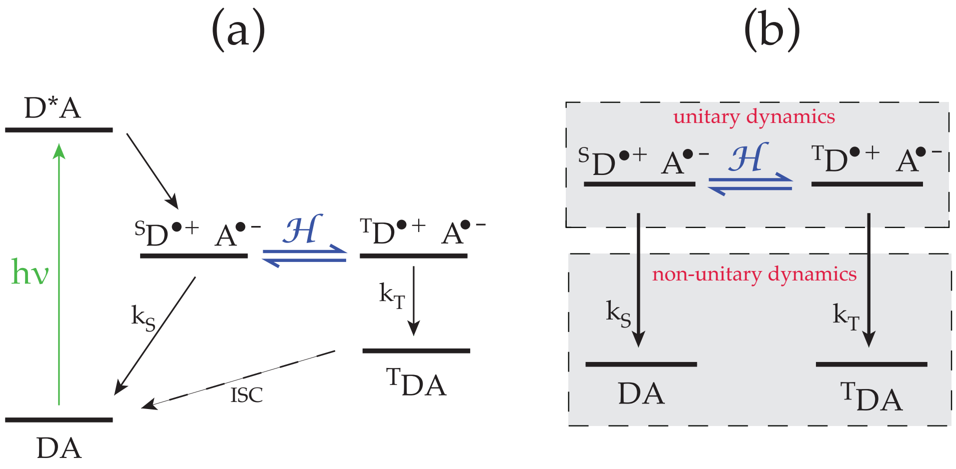

FIGURE 2.1: (a) Simplified energy level diagram depicting radical-ion pair reaction dynamics. A donor-acceptor dyad is photo-excited and a subsequent charge transfer produces a singlet radical-ion pair. Magnetic interactions within the radical pair induce coherent singlet-triplet mixing, while spin-dependent charge recombination leads to singlet-triplet neutral products at the respective reaction rates k_S and k_T. The reaction can, in principle, close through intersystem crossing from the triplet to the singlet ground state. (b) Simplified version of (a) neglecting the photo-excitation and charge transfer steps. Both diagrams could be misleading if taken too literally, since they might suggest that e.g. only singlet RP's recombine to singlet neutral products. This is not the case, since a radical-ion pair in a coherent S-T superposition can recombine into e.g. a singlet neutral product.

The dimension of the density matrix ρ is $d = 4\prod_{n=1}^{M}(2I_n+1)$ where I_n is the nuclear spin of the nth nucleus, with $n = 1, 2, ...M$. We define two orthogonal projector operator namely Q_S and Q_T where they spam the electron singlet and triplet subspace and the role of them is to project the RP system to this subspace. These operators are described by $d \times d$ matrices which satisfy the conditions $(Q_j)^2 = Q_j$,$Q_S + Q_T = I$ and $Q_S Q_T = 0 = Q_T Q_S$ where I is the $d \times d$ unity matrix, 0 is the $d \times d$ zero matrix and $j = S, T$. The two operators are defined as: $Q_S = \frac{1}{4} - \vec{s}_D \cdot \vec{s}_A$ and $Q_T = \frac{3}{4} + \vec{s}_D \cdot \vec{s}_A$ where $\vec{s}_D$ and $\vec{s}_A$ are the spin operators of the donor and acceptor respectively, written as proper dimensional matrices like: $s_{jA} = s_j \otimes I_2 \otimes ... \otimes I_{2I_M+1}$. Using the definitions above we express all the quantities of interest in the uncoupled many spin-1/2 basis. Another way to define the above operators, which is more simple and straightforward, is by first defining the singlet-triplet spin states.

$$|S\rangle = \frac{1}{\sqrt{2}}(|AB\rangle - |BA\rangle) \tag{2.1}$$

$$|T_0\rangle = \frac{1}{\sqrt{2}}(|AB\rangle + |BA\rangle) \tag{2.2}$$

$$|T_+\rangle = |AA\rangle \tag{2.3}$$

$$|T_-\rangle = |BB\rangle \tag{2.4}$$

where $|A\rangle$ denotes the eigenstate of a spin-1/2 operator which the spin to the eigenstate with the largest eigenvalue along the quantization axis, while $|B\rangle$ denotes the eigenstate which corresponds to the smallest eigenvalue of the spin along the quantization axis. In this way, the projector operators take the simple form:

$$Q_S = |S\rangle \langle S| \tag{2.5}$$

and

$$Q_T = \sum_{q=\pm,0} |T_q\rangle \langle T_q| \tag{2.6}$$

where one have to be careful to expand correctly the above matrices in the case where nuclear spins are included. As it is depicted in Figure 2.1 there are also the rates k_S and k_T to consider where if there are not magnetic interactions ($H = 0$) and the radical pair is in singlet (triplet) state then the population would decay exponentially at rates k_S (k_T).

2.2 The Hamiltonian

The Hamiltonian that drives the coherent singlet-triplet mixing of the radicals, in the most general case contains the electron Zeeman interactions, the hyperfine interactions between the electron and the nuclear spins, the dipole-dipole interaction and the spin exchange interaction between the two electron spins and the nuclear Zeeman interactions that are much smaller than the electron ones. For simplicity, we suppose that couplings between the donor's spins and the acceptor's ones are of no importance in the RP dynamics. The **Zeeman Interaction** of the two electrons ($n = 1, 2$) with the external magnetic field (for example Earth's magnetic field $\left|\vec{B}\right| \approx 50\mu\text{T}$)is given by:

$$H_{Zee} = \sum_{n=1}^{2} \mu_{\text{B}} g_n \vec{B} \cdot \vec{s}_n \tag{2.7}$$

where μ_{B} is Bohr's magneton, g_n is the g-factor of each electron and $\vec{s}_n$ is the electron spin operators that are coupled with the constant magnetic field. The **hyperfine interaction** is of the form:

$$H_{hyp} = \sum_{n=1}^{2} \sum_{m=1}^{M} \mu_{\text{B}} g_n \vec{s}_n \cdot \overset{\leftrightarrow}{A}_{n,m} \cdot \vec{I}_{n,m} \tag{2.8}$$

and it couples the two electrons with the M nuclear spins at each site (donor-acceptor site). The nuclear spin operators are denoted as $\vec{I}_{n,m}$ while the coupling tensor is a second rank tensor that accounts for the geometry of the coupling and is generally expressed with a matrix of the form:

$$\overset{\leftrightarrow}{A} = \begin{pmatrix} A_{xx} & A_{xy} & A_{xz} \\ A_{yx} & A_{yy} & A_{yz} \\ A_{zx} & A_{zy} & A_{zz} \end{pmatrix} \tag{2.9}$$

For the most of the calculations in this thesis we used isotropic hyperfine interactions with the same strength for the three axes i.e.

$$\overleftrightarrow{A} = \begin{pmatrix} A_{xx} & A_{xy} & A_{xz} \\ A_{yx} & A_{yy} & A_{yz} \\ A_{zx} & A_{zy} & A_{zz} \end{pmatrix} = \begin{pmatrix} A_{xx} & 0 & 0 \\ 0 & A_{yy} & 0 \\ 0 & 0 & A_{zz} \end{pmatrix} = A_{xx} \begin{pmatrix} 1 & 0 & 0 \\ 0 & 1 & 0 \\ 0 & 0 & 1 \end{pmatrix} \tag{2.10}$$

We suppose that the electron's wavefunction, overlaps only with the nucleus of the same molecule, thus, there are no hyperfine interactions between for example, the donor's electron and the acceptors nucleus. In other words there is no electron's wavefunction overlap between donor and acceptor. In bibliography, this is known as Fermi's contact interaction.

The **electron spin exchange term** can be neglected for sufficiently large distances between the two molecules when the electronic wavefunctions does not overlap. This interaction scales as: $\mathcal{O}(e^{-|\vec{r}|})$ where $|\vec{r}|$ is the spatial distance between the two spins.

The **nuclear Zeeman interaction** is three orders of magnitude smaller than the electron Zeeman interaction due to the fact that $\frac{m_p}{m_e} \approx 1836$.

Finally, the **dipole-dipole magnetic interaction** depends also on the distance between the two spins and is of the form:

$$H_{Dip} = -\frac{\mu_0 \gamma_1 \gamma_2 \hbar^2}{4\pi |\vec{r}|^3} (3(\vec{s}_1 \cdot \hat{r})(\vec{s}_2 \cdot \hat{r}) - \vec{s}_1 \cdot \vec{s}_2) \tag{2.11}$$

Thus it scales as $\mathcal{O}(\frac{1}{|\vec{r}|^3})$ thus is also negligible.

2.3 Master Equations

In closed quantum systems, the evolution of a density matrix is, as we say ,unitary (conserves the total probability),is generated by the Hamiltonian and is given by the von Neumann equation in differential form:

$$\frac{d\rho}{dt} = -\frac{i}{\hbar}[H, \rho] \tag{2.12}$$

It describes the evolution of an ensemble of quantum objects completely isolated from their environment. When there is interaction with the environment or there is some population loss from the system then the evolution of the density matrix is given usually by a unitary Hamiltonian term and a term that account for the interaction or the population loss. Thus the equation that describes the evolution takes the form:

$$\frac{d\rho}{dt} = -\frac{i}{\hbar}[H, \rho] + G(\rho) \tag{2.13}$$

In the theory of open quantum systems, where interaction with the environment dissipates the coherent dynamics that is generated from the Hamiltonian and in the Markov approximation, where the environment "forgets" the effect from the system instantly, the $G(\rho)$ has a very characteristic form and the whole master equation is, as we say, in Lindblad form:

$$\frac{d\rho}{dt} = -\frac{i}{\hbar}[H,\rho] + \sum_n \frac{k_n}{2}(L_n^\dagger L_n\rho - \rho L_n^\dagger L_n + L_n\rho L_n^\dagger) \tag{2.14}$$

2.3.1 Haberkorn's Master Equation

In the Radical-Pair system, the time evolution of the density matrix ρ has been traditionally described [24] by Haberkorn's master equation (HME) which is a phenomenological equation given from:

$$\frac{d\rho}{dt} = -i[H,\rho] - \frac{k_S}{2}(Q_S\rho + \rho Q_S) - \frac{k_{\mathrm{T}}}{2}(Q_{\mathrm{T}}\rho + \rho Q_{\mathrm{T}}) \tag{2.15}$$

The first term of HME is the ordinary unitary evolution driven by the Hamiltonian H which usually contains the magnetic interactions (Zeeman, hyperfine, etc). As singlet and triplet states are not eigenstates of H. this term generates S-T coherence. The second term describes the population decay in a spin selective way. This master equation describes mathematically the reaction cycle of Figure 2.1. In the following, we plot the mean value of the operator Q_T as a function of time first in the case of unitary evolution only with the Hamiltonian while in the second case we use the whole master equation .As we can see, there is a coherent singlet-triplet mixing in the first case which is dissipated exponentially by the spin dependent population loss of the radicals in the second plot.

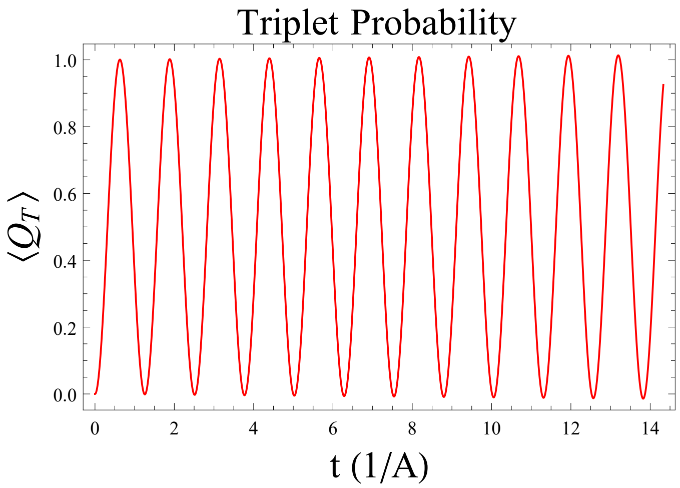

FIGURE 2.2: Mean value of the operator Q_T as a function of time in the parameter regime where $\omega = 1, A = 10, k_S = \frac{\omega}{4}, k_T = \omega$ using Hamiltonian evolution with $H = \omega(s_{1,x} + s_{2,x}) + As_{1,x}I_{1,x}$ and supposing only one nuclear spin in hyperfine interaction.

It is obvious that, when the rates k_S and k_T are much larger than the Rabi frequency between the singlet-triplet states then the Hamiltonian evolution is almost surpassed by the recombination process. In Haberkorn's case and also in Kominis' , as we will see, the population is lost from the system in a rate:

$$\frac{dTr\{\rho\}}{dt} = -k_S Tr\{\rho Q_S\} - k_T Tr\{\rho Q_T\} \tag{2.16}$$

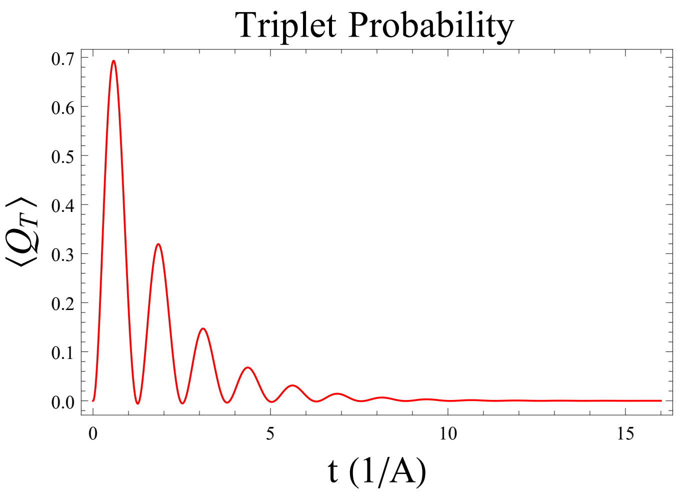

FIGURE 2.3: Mean value of the operator Q_T as a function of time in the parameter regime where $\omega = 1, A = 10, k_S = \frac{\omega}{4}, k_T = \omega$ using Haberkorn's master equation with the Hamiltonian $H = \omega(s_{1,x} + s_{2,x}) + A s_{1,x} I_{1,x}$ and supposing only one nuclear spin in hyperfine interaction.

2.3.2 Kominis' Master Equation

The master equation derived by Kominis [10-12] reads:

$$\begin{gathered}\frac{d\rho}{dt} = -i[H,\rho] \\ -\frac{k_S + k_T}{2}(Q_S\rho + \rho Q_S - 2Q_S\rho Q_S) \\ -(1 - p_{coh})(k_S Q_S \rho Q_S + k_T Q_T \rho Q_T) \\ -p_{coh}\frac{dr_S + dr_T}{dt}\frac{1}{Tr\{\rho\}}(Q_S\rho Q_S + Q_T\rho Q_T + \frac{1}{p_{coh}}Q_S\rho Q_T + \frac{1}{p_{coh}}Q_T\rho Q_S)\end{gathered} \tag{2.17}$$

S-T coherence is generated by H, dissipated by the Lindblad term (second term) ,which formally derived in [10,13], and quantified by p_{coh}, which is a map of the density matrix onto the interval [0,1], defined in [3]. At the single radical-pair level, this term is translated into unobserved randomly occurring projections of the radical pair state ρ to either the singlet RP state $\frac{Q_S\rho Q_S}{Tr\{\rho Q_S\}}$ with probability $dp_S = \frac{k_S+k_T}{2}dtTr\{\rho Q_S\}$ or to the triplet RP state: $\frac{Q_T\rho Q_T}{Tr\{\rho Q_T\}}$ with probability $dp_T = \frac{k_S+k_T}{2}dtTr\{\rho Q_T\}$. That the second term dissipates the S-T coherence can be seen by general decomposition of the RP density matrix as $\rho = \mathrm{I}\rho\mathrm{I} = (Q_S + Q_T)\rho(Q_S + Q_T) = Q_S\rho Q_S + Q_T\rho Q_T + Q_S\rho Q_T + Q_T\rho Q_S$. The first two terms account for singlet and triplet PR population, while the last two terms account for S-T coherence. When can thus rewrite the Lindblad term in the form: $-\frac{k_S+k_T}{2}(Q_S\rho Q_T + Q_T\rho Q_S)$ i.e. this term removes the S-T coherent part of the density matrix at a rate $-\frac{k_S+k_T}{2}$. The two last terms of the master equation are the reaction terms, reducing the RP population, given by $Tr\{\rho\}$, in a spin-selective way, and derived in [12] using the theory of quantum retrodiction.

For both theories the fraction of the RP population recombining into singlet and triplet neutral products within the interval dt is $dr_S = k_S dt Tr\{\rho Q_S\}$

and $dr_T = k_T dt Tr\{\rho Q_T\}$, respectively. A schematic representation of Kominis master equation is given in Figure 2.2.

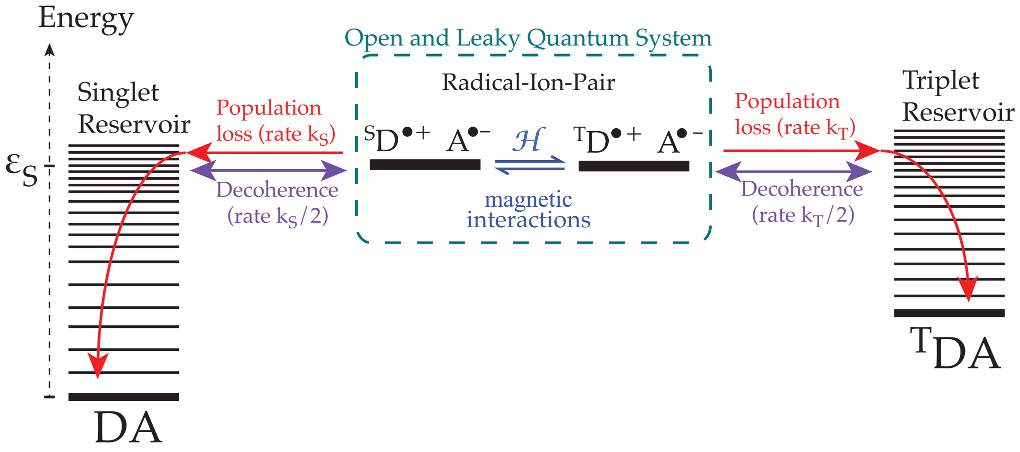
Energy
Open and Leaky Quantum System
Radical-Ion-Pair
Singlet Reservoir
Triplet Reservoir
Population loss (rate k_S)
Population loss (rate k_T)
$^S D^{\bullet +}$ $A^{\bullet -}$
$\mathcal{H}$
$^T D^{\bullet +}$ $A^{\bullet -}$
ε_S
Decoherence (rate $k_S/2$)
Decoherence (rate $k_T/2$)
magnetic interactions
DA
$^T DA$

FIGURE 2.4: Detailed energy level structure of radical-ion pairs. The vibrational excitations of the singlet $^S DA$ and the triplet $^T DA$ ground state form a reservoir that probes the electron spin state of the RP, leading to an intramolecule measurement of Q_S. Virtual transitions with rates $\frac{k_S}{2}$ and $\frac{k_T}{2}$ to the reservoir levels and back to the RP lead to S-T decoherence, while real transitions with rates k_S and k_T to the reservoir states followed by their decay to the ground state leads to recombination.

Haberkorn's theory considers p_{coh} to be always zero, i.e. it is a limiting case of Kominis theory valid in the regime of strong spin relaxation, where S-T coherence decays in a time scale much faster than $\frac{1}{k_S+k_T}$. However, the difference between the two theories can be best elucidated by considering single radical-pair quantum trajectories. Such an analysis held in [14]. If one assumes, as has been the intuitive understanding in spin chemistry, that RP's only undergo unitary evolution until they recombine the HME qualitatively and quantitatively disagrees with the quantum-trajectory average. However, one could decide to question the results of this quantum trajectory analysis, as was done in [28], albeit unsuccessfully [29]. The following provides an independent demonstration of HME's failure based on entropy of quantum systems.

Before proceeding, we note (i) the case of RP's with equal recombination rates is particularly innocuous. Setting $k_S = k_T = k$ in HME, it is trivial to show that its solution is $\rho(t) = e^{-kt}R(t)$ where $R(t)$ satisfies the equation: $\frac{dR}{dt} = -i[H, R]$. That is, the densisty matrix R undergoes unitary and clearly physical evolution, while the RP density matrix $\rho(t)$ describes the exact same physical state as R but having an exponentially decaying population. Similarly, Kominis master equation leads again to $\rho(t) = e^{-kt}R(t)$ but now $R(t)$ satisfies the Lindblad equation $\frac{dR}{dt} = -i[H, R] - k(Q_S R + R Q_S - 2 Q_S R Q_S)$, which again is a physically acceptable law [31] of evolving a density matrix. Hence, in the special case of $k_S = k_T$, both theories produce physically acceptable evolution laws, so we do not expect any of them to violate any entropy bound. The problems with HME arise as soon as $k_S \neq k_T$. Physically,this is a very interesting parameter regime as it appears in photosynthetic reaction centers [22]. In the following we will thus focus in the case $k_S \neq k_T$.(ii) HME keeps an initially pure state pure all the time. This can be easily proved by showing that all time-derivatives of $\pi(t) = \frac{Tr\{\rho^2\}}{Tr\{\rho\}^2}$ are zero when evaluated at $t = 0$. In contrast, Kominis theory evolves an initially pure state into a mixture due to the Lindblad dephasing term. To be able to compare the two theories,we add a small spin-randomizing term of the form $-\gamma(\rho - \frac{\mathrm{I}}{Tr\{I\}}Tr\{\rho\})$.

Since the population of the RP's, given by $Tr\{\rho\}$, is time-dependent, with $Tr\{\rho\} = 1$ at $t = 0$ and $Tr\{\rho\} = 0$ at $t \to \infty$, the single-radical-pair state at time t is $\frac{\rho}{Tr\{\rho\}}$.

Chapter 3

Entropy of Quantum Systems: The Radical-Pair System

3.1 Quantum Measurement and Entropy

The scope of this thesis is to apply the Ozawa Entropy bound and the Lanford-Robinson bound in the radical-pair system. Before doing so, we have to acquire an intuitive understanding of quantum measurement theory and its applications, thus in this chapter,first of all, we will discuss the source of these bounds then we will apply them to a simple system such as a spin-1 particle to get an intuitive understanding on the way that these bounds work and finally we will apply them to the two radical-pair master equations described in Chapter 2. The traditional theory of quantum measurement established by thought experiments of Bohr and von Neumann was based on the interaction of a quantum system with a classical apparatus. Recently this picture has changed and the idea of modern quantum measurement theory is that interactions between different quantum systems ,with arbitrary many degrees of freedom, can be described as a quantum measurement process. Usually the interaction between the two systems is described by a Hamiltonian H_{int} which contains operators from both interacting systems. The most common and simple quantum measurement that can be made on a quantum system system is the von Neumann measurement. This kind of measurement is described by a set of projector operators $\{|n\rangle\langle n|\}$ which project a system described by a density matrix ρ to an eigenstate of this operator. One can show that all possible measurements that can be made on a quantum system can be derived from the von Neumann measurement. In order to do so, we will use a quantum system with dimension N as our "target" system and a quantum system of dimension M as our "probe" system. The two systems are prepared in two different states, one independent of the other. The idea is that we let the two systems interact,thus, they become correlated and entangled and then we make von Neumann measurements to the probe system. In this way we gain information about the target system of interest. We denote the basis that we measure the probe as $\{|n\rangle\}, n = 0, ..., M-1$. For simplicity and without loss of generality we choose the probe system to be in the ground state i.e. $\rho_{probe} = |0\rangle\langle 0|$ thus at time $t = 0$ the combined density matrix is

$$\rho_{comb} = \rho_{probe} \otimes \rho_{target} = |0\rangle\langle 0| \otimes \rho_{target} \tag{3.1}$$

The interaction between the two systems may be described by a unitary operator that acts in the joint space of both systems. Since U acts in the tensor-product space, it can be written in the matrix form:

$$U = \sum_{nn'kk'} u_{nn'kk'} \left|n\right\rangle \left|s_k\right\rangle \left\langle n'\right| \left\langle s_{k'}\right| \tag{3.2}$$

or in a more compact form:

$$U = \sum_{nn'} \left|n\right\rangle \left\langle n'\right| \otimes A_{nn'} \tag{3.3}$$

where

$$A_{nn'} = \sum_{kk'} u_{nn'kk'} \left|s_k\right\rangle \left\langle s_{k'}\right| \tag{3.4}$$

It is clear that $\left|s_k\right\rangle$ is a set of basis states for the target system. Since U is unitary matrix it should be true that $U^\dagger U = I$ this immediately implies a condition on the the A matrices of the form:

$$I = \sum_n A_n^\dagger A_n \tag{3.5}$$

where $A_n \equiv A_{0n}$ for short-hand. Any set of operators that satisfy the above condition can describe a possible quantum measurement on the system. This is because the above equation is sufficient to ensure that there exists a unitary matrix U with all the good properties. We now apply the unitary interaction U to the initial state of the two systems and then project the probe system onto the state $\left|n\right\rangle$ using a von Neumann projection. The final state is:

$$\rho(t)_{comb} = \overbrace{(\left|n\right\rangle \left\langle n\right| \otimes I)}^{\Pr ojector} \underbrace{U(\left|0\right\rangle \left\langle 0\right| \otimes \rho_{target})U^\dagger}_{Interaction} \overbrace{(\left|n\right\rangle \left\langle n\right| \otimes I)}^{\Pr ojector} \tag{3.6}$$

using Eq.(3.3) we immediately obtain $\rho(t)_{comb} = \left|n\right\rangle \left\langle n\right| \otimes A_n^\dagger \rho_{target} A_n$ thus the final state of the target is

$$\tilde{\rho}_n^{target} = \frac{A_n^\dagger \rho_{target} A_n}{Tr\{A_n^\dagger \rho_{target} A_n\}} \tag{3.7}$$

and the probability of obtaining the above state is given by:

$$p_n = Tr\{A_n^\dagger A_n \rho_{target}\} \tag{3.8}$$

The above derivation is based on [27].Besides measuring the probe system using a von Neumann measurement, one could also trace out the probe's degrees of freedom from the compound target-probe system. This is like taking an average over all the von Neumann measurement outcomes.

$$\rho_{target}(t) = Tr_E\{U(\left|0\right\rangle \left\langle 0\right| \otimes \rho_{target})U^\dagger\} = \sum_M \left\langle M\right| U \left|0\right\rangle \rho_{target} \left\langle 0\right| U^\dagger \left|M\right\rangle$$

$$\equiv \sum_M \hat{M}_M \rho_{target} \hat{M}_M^\dagger \tag{3.9}$$

where the operators $M = \langle M| U |0\rangle$ are named Kraus operators. Supposing that the system is initially in a pure state we have:

$$\rho_{target}(t) = \sum_M \hat{M}_M |s\rangle \langle s| \hat{M}_M^\dagger = \sum_M \left|\tilde{\Psi}_\mathrm{M}\right\rangle \left\langle \tilde{\Psi}_\mathrm{M}\right| \tag{3.10}$$

where $\left|\tilde{\Psi}_\mathrm{M}\right\rangle \equiv M_M |s\rangle$ and the tilda is to remind us that the states are in general not normalized and not orthogonal to each other. We can normalize the states in the following way:

$$|\Psi_\mathrm{M}(t)\rangle = \frac{\left|\tilde{\Psi}_\mathrm{M}(t)\right\rangle}{\left\|\tilde{\Psi}_\mathrm{M}(t)\right\|} \tag{3.11}$$

where,

$$\left\|\tilde{\Psi}_\mathrm{M}(t)\right\|^2 = \left\langle \tilde{\Psi}_\mathrm{M}(t)\right| \left|\tilde{\Psi}_\mathrm{M}(t)\right\rangle = \langle \Psi_\mathrm{M}(0)| M_M^\dagger M_M |\Psi_\mathrm{M}(0)\rangle \equiv P_M(t) \tag{3.12}$$

Substituting this back to equation (3.10) we can see that:

$$\rho_{target}(t) = \sum_M \left|\tilde{\Psi}_\mathrm{M}\right\rangle \left\langle \tilde{\Psi}_\mathrm{M}\right| = \sum_M P_M(t) |\Psi_\mathrm{M}(t)\rangle \langle \Psi_\mathrm{M}(t)| \tag{3.13}$$

which is a mixed state. The conclusion is that, we start initially with a pure state with zero entropy (by definition pure states have zero entropy) and after the interaction of the target system with the environment, the system's state is a mixed state with non-zero entropy.Thus there is a production of entropy due to the interaction. It is not difficult to show in the same way that there is also generation of entanglement due to the interaction but this is irrelevant for this thesis. Since we know how to describe a quantum measurement in terms of the measurement operators we here introduce the Ozawa bound as introduced by Ozawa [25] and later by Jacobs [27]. Consider a system described by the density matrix ρ. If an efficient quantum measurement is performed, with the possible post-measurement states $\tilde{\rho}_n$ occurring with probabilities p_n, then

$$\overbrace{\sum_n p_n S\left[\tilde{\rho}_n\right] \leq S\left[\rho\right]}^{Ozawa} \tag{3.14}$$

where $S\left[r\right] = -Tr\{r \ln r\}$ is the von Neumann entropy of the density matrix r. The interpretation is that our ignorance after the measurement averaged over the possible measurement results, $\sum_n p_n S\left[\tilde{\rho}_n\right]$, should be smaller than our initial ignorance about the system, $S\left[\rho\right]$, if we are to extract information about the system.Another interpretation is that the average amount of information that we get from these measurements must be smaller or equal to the total amount of information that the system contains. To get an insight into the quantum measurements and the Ozawa bound, in the next section, we illustrate an example with a simple spin-1 system.

3.2 The Spin-1 Paradigm

We here provide an intuitive understanding of the Qzawa bound using a simple spin-1 system evolving under the influence of a magnetic field and a continuous quantum measurement. We consider a spin-1 initially in the state $|1\rangle$, the $m = 1$ eigenstate of s_z, residing in a constant magnetic field along the x-axis, i.e. the Hamiltonian is $H = \omega s_x$. A continuous quantum measurement is performed at a rate . We remind the reader that every set of operators L_n satisfying the condition $\sum\limits_n L_n^\dagger L_n = I$ describes a possible quantum measurement, the possible measurement results being $\tilde{\rho}_n = \frac{L_n \rho L_n^\dagger}{p_n}$ with probability $p_n = Tr\{\rho L_n^\dagger L_n\}$. We here take $L = |1\rangle\langle 1|$, and as measurement operators $L_1 = \sqrt{\kappa dt} L$, $L_2 = \sqrt{\kappa dt}(I - L)$ and $L_3 = \sqrt{1 - \kappa dt}(I - iHdt)$. Since L and $I - L$ are Hermitian operators, it is easily seen that the condition $L_1^\dagger L_1 + L_2^\dagger L_2 + L_3^\dagger L_3 = I$ is satisfied.

If the spin's state is ρ_t at time t, then in the following time interval dt the spin is transformed into the state $\tilde{\rho}_j = \frac{L_j \rho L_j^\dagger}{Tr\{\rho L_j^\dagger L_j\}}$ with probability $p_j = Tr\{\rho L_j^\dagger L_j\}$. Since $\sum\limits_n L_n^\dagger L_n = I$, it follows that $\sum\limits_j p_j = 1$. Writing $\rho_{t+dt} = \sum\limits_j p_j \tilde{\rho}_j$, we find the expected Lindblad equation $\frac{d\rho}{dt} = \frac{\rho_{t+dt} - \rho_t}{dt} = -i[H, \rho] - \kappa(L\rho + \rho L - 2L\rho L)$.

The ensemble of spins described by ρ at time t is a mixture consisting of those spins that have evolved unitarily and those that at some earlier time have been projected by either L or $I - L$. The mixture has a non-zero von Neumann entropy $S_{initial} = S[\rho]$. Now, among those dt spins that have undergone a measurement during dt, a fraction $p = Tr\{\rho L\}$ and $1 - p$ end up in the state $\tilde{\rho}_1$ and $\tilde{\rho}_2$, respectively. Hence the entropy of the measurement results is $S_{final} = -pTr\{\tilde{\rho}_1 \ln \tilde{\rho}_1\} - (1 - p)Tr\{\tilde{\rho}_2 \ln \tilde{\rho}_2\}$. According to the Qzawa bound, it should be $S_{final} \le S_{initial}$. This is the case, as shown in Fig.3.1.(a). Furthermore, the Lanford-Robinson bound states that the positive (according to Ozawa) difference $S_{initial} - S_{final}$, which is the information gain from the measurement, cannot be larger than the Shannon information of the probability distribution defined by p and $1 - p$ i.e.

$$\underbrace{S_{initial} - S_{final} \le H[p]}_{Lanford-Robinson} \tag{3.15}$$

where $H[p] = -p \log p - (1 - p) \log(1 - p)$. Again, this bound is also satisfied as shown in Fig.3.1.(b), the Lanford-Robinson bound is saturated at those times when the spin is in an eigenstate of the measurement operator L, which should be expected, since the information extraction is optimal.

Finally, as shown in Fig.3.1.(c), the spin precesses on the $y - z$ plane, spiralling towards the maximally mixed state with matrix elements $\rho_{ij} = \frac{\delta_{ij}}{3}$. Thus,the entropy of ρ should tent to $Log(3)$. Moreover, the fraction of spins projected to $|1\rangle\langle 1|$tends to $1/3$, hence the fraction of spins projected to the space spanned by $|0\rangle$ and $|-1\rangle$ tends to $2/3$. The state of the latter tends to the fully mixed $2x2$ density matrix having entropy $Log(2)$., hence the final entropy (the state $|1\rangle\langle 1|$ is pure and has zero entropy) tends to $\frac{2}{3}Log(2)$. Finally, as the state is diagonal at $t \to \infty$, the extracted information is maximal and equal to Shannon's information, which is $H\left[\frac{1}{3}\right]$.

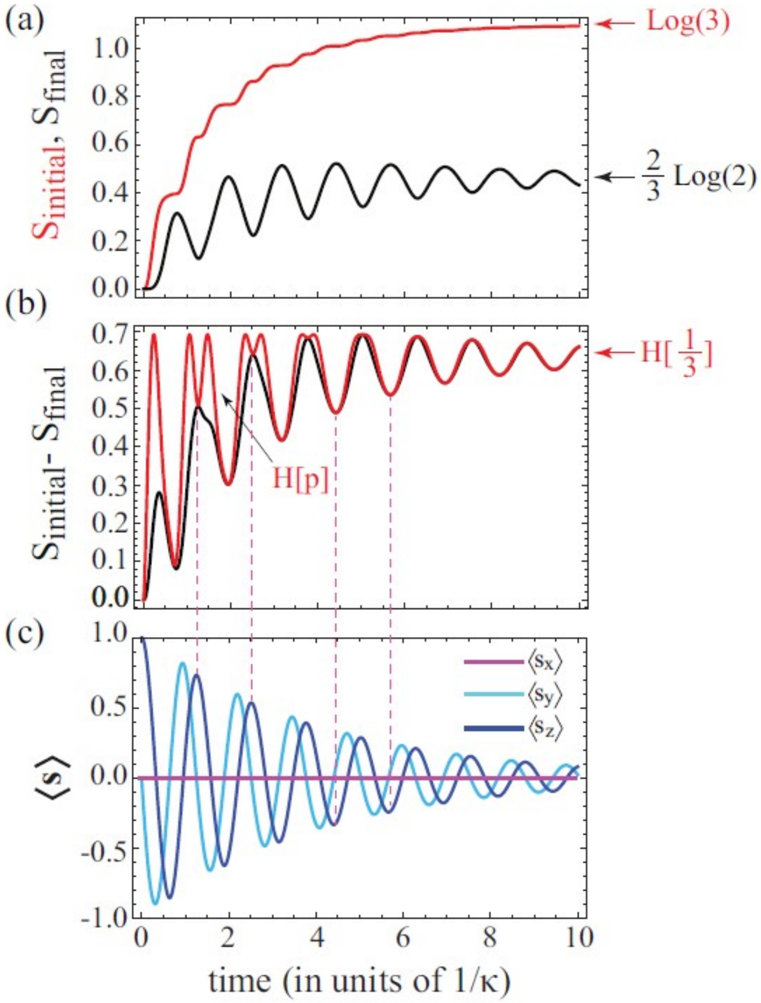

FIGURE 3.1: Spin-1 precessing in a magnetic field under the influence of a continuous quantum measurement with the projector $L = |1\rangle\langle 1|$.(a) Average entropy of the measurement outcomes(black line) is lower than the entropy of the pre-measurement spin state(red line),as dictated by the Ozawa bound.(b) The difference is smaller than the information content of the spin state, as dictated by the Lanford-Robinson bound. (c) Spin expectation values as a function of time, approaching the maximally mixed state $\rho_{ij} = \frac{\delta_{ij}}{3}$ having $\langle s_x\rangle = \langle s_y\rangle = \langle s_z\rangle = 0$. The measurement rate was $\kappa = \omega/5$.

3.3 Ozawa Entropy bound and the Radical-Pair Mechanism

3.3.1 Haberkorn's Master Equation Violates the Ozawa Entropy Bound

The spin-1 example was a very good illustration of the Ozawa bound and gave us a good insight of how these bounds apply. Here we apply the same bounds to the more complicated system of radical-ion pairs. To do so we remind that the single-radical-pair state at time t is $\frac{\rho}{Tr\{\rho\}}$ and hence the von

Neumann entropy of the radical-pairs prior to the measurement is $S_{initial} = S\left[\frac{\rho}{Tr\{\rho\}}\right]$. From Kominis theory's perspective, during the time interval dt at time t there will be dr_S singlet and dr_T triplet neutral products, as well as dp_S and dp_T projections to the singlet and triplet RP states, respectively. For both cases the respective spin states are $\rho_S = \frac{Q_S \rho Q_S}{Tr\{\rho Q_S\}}$ and $\rho_T = \frac{Q_T \rho Q_T}{Tr\{\rho Q_T\}}$, only in the latter case the electron is localized back in the donor, which is irrelevant for the spin state entropy. Hence

$$S^K_{final} = \frac{dr_S + dp_S}{dr_S + dr_T + dp_S + dp_T} S\left[\rho_S\right] + \frac{dr_T + dp_T}{dr_S + dr_T + dp_S + dp_T} S\left[\rho_T\right] \tag{3.16}$$

From Haberkorn's theory perspective, there are only singlet and triplet neutral products produced during dt, hence

$$S^H_{final} = \frac{dr_S}{dr_S + dr_T} S\left[\rho_S\right] + \frac{dr_T}{dr_S + dr_T} S\left[\rho_T\right] \tag{3.17}$$

The reduction in the post-measurement entropy compared to the pre-measurement is about the information conveyed by the measurement. According to the Lanford-Robinson bound [26,27], this information is bound by the Shannon entropy of the pre-measurement state: $S_{initial} - S_{final} \leq H\left[q_S\right]$ where $q_S = \frac{Tr\{\rho Q_S\}}{Tr\{\rho\}}$ and $q_T = 1 - q_S$ are the probabilities that the radical-pair is in the singlet or triplet state, respectively and $H\left[q_S\right] = -q_S \log q_S - (1 - q_S)\log(1 - q_S)$.

We consider a radical-ion pair with one nuclear spin having isotropic hyperfine coupling with e.g. the donor's unpaired electron. In Fig.3.2.(a) we show Haberkorn's prediction for $S_{initial}$ and S_{final}. Evidently, the Ozawa bound is violated, hence the difference $S_{initial} - S_{final}$ being negative, it is meaningless to test the Lanford-Robinson bound. In Fig.3.2.(b),(c) we show the results of Kominis master equation, which satisfies both Ozawa and Lanford-Robinson bounds.

To understand the root of Haberkorn's violation, we note that S_{final} is similar in both theories. Hence the root of the violation in the former is the underestimation of $S_{initial}$. For the sake of this explanation we omit the rate k_S, since anyhow we consider the case $k_T >> k_S$. It follows from HME that the coherence $Q_S \rho Q_T + Q_T \rho Q_S$ decays at the rate $\frac{k_T}{2}$, whereas the population $Q_T \rho Q_T$ decays at rate k_T. Thus the coherence decays just due to the population loss, i.e. there is no intrinsic dissipation of coherence, and therefore an initially pure state remains pure. In contrast, from Kominis theory it follows that the coherence is dissipated at the rate $k_T[1/2 + q_T] \geq k_T/2$, whereas population decays at the rate $k_T[1 + p_{coh}(q_T - 1)] \leq k_T$ (obviously $0 \leq q_T \leq 1$). Thus the coherence is faster than what would result just due to population loss,which makes for the entropy production.

On a more abstract level, HME fails to account for the fact that radical-pair recombination essentially is a rate process conditioned on the quantum state of the molecule. To understand this subtle point consider two-level atoms (with two long-lived states $|g\rangle$ and $|e\rangle$) escaping a box with a hole, if they are in the $|g\rangle$ state. The hole's diameter determines the escape rate (the equivalent of the recombination rates). However, every time the atom approaches the hole, some physical process must measure the atom's state,which in general could be in any coherent superposition of $|g\rangle$ and $|e\rangle$.

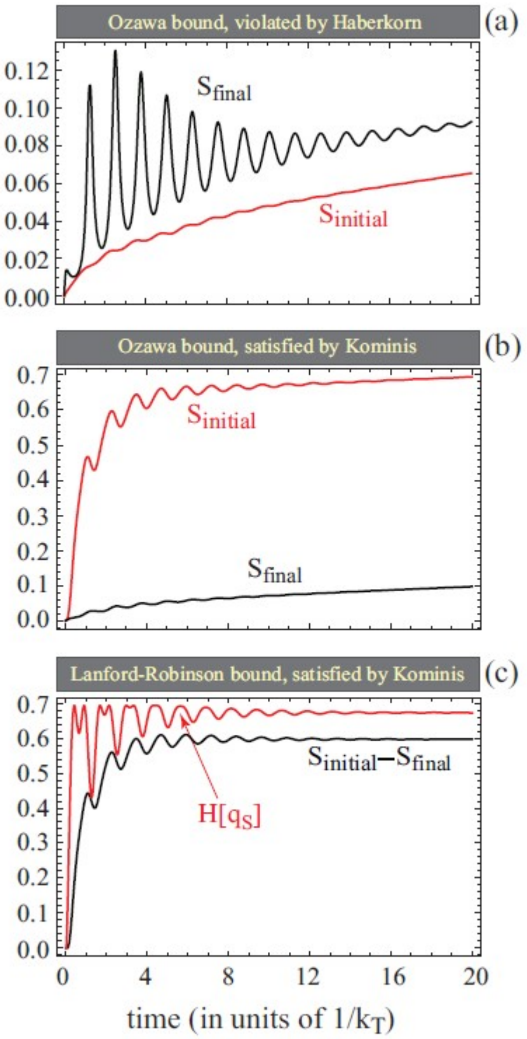

FIGURE 3.2: The simulations were performed with an isotropic Hamiltonian $H = A\vec{I}\cdot\vec{s}_D$, asymmetric recombination rates, $k_S = A/100$ and $k_T = A/5$,a randomizing term with γ = A/2000 and initial state $|S\rangle \otimes |\uparrow\rangle$.

If the result of this measurement is positive, the atom will escape with a given probability. It is this measurement (the equivalent of the state projections leading to S-T dephasing in our theory) that is an entropy source for the atoms remaining in the box.

Besides serving as a test of the master equation, the quantum information approach to RP reactions is useful in its own right. This is because, by definition, it carries in an abstract way the full information that can be extracted from the reaction by any kind of measurement. To define the extracted information relevant to metrology, we first note that the RPs being projected to the singlet and triplet neutral subspaces, with the respective probabilities dp_S and dp_T, are not physically accessible as are the singlet and triplet neutral products. In other words, the actual information that can be extracted along the reaction is determined by the change in entropy of those $dr_S + dr_T$ radical pairs which lead to the dr_S singlet and dr_T triplet neutral reaction products.We thus define the integrated extracted information by:

$$I_{ex} = \int \{(dr_S + dr_T + dp_S + dp_T)S_{initial} \\ -(dr_S + dp_S)S[\rho_S] - (dr_T + dp_T)S[\rho_T]\} \tag{3.18}$$

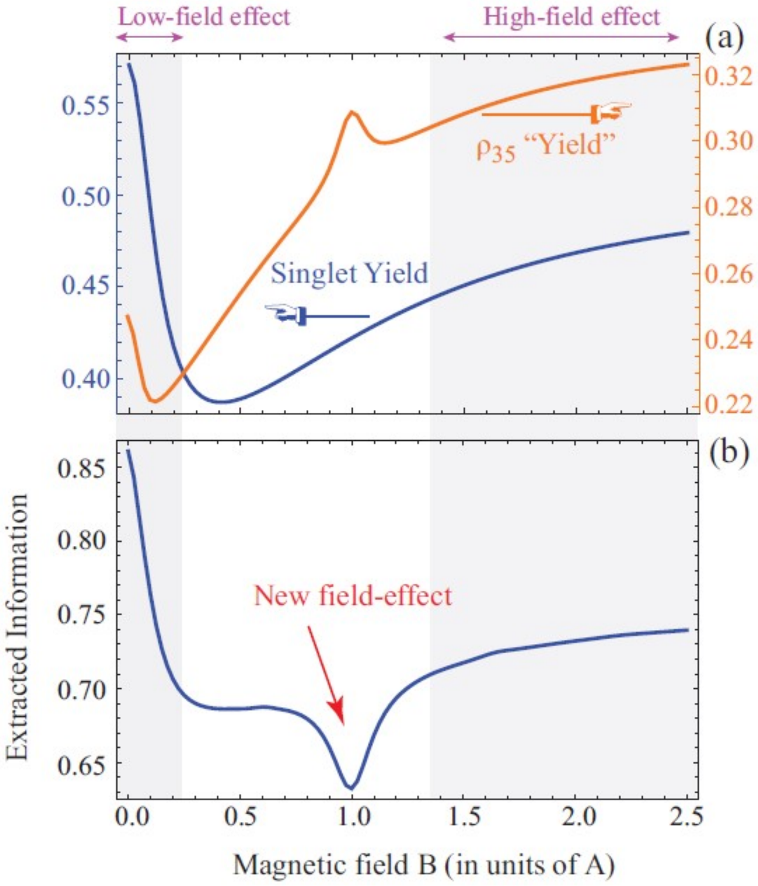

FIGURE 3.3: (a) Singlet reaction yield dependence (left y-axis) on the magnetic field, depicting low- and high-field effects. (b) Extracted information $I_{ex}(B)$ exhibits both low- and high-field effect, but also reveals a new field-effect at $B = A$. This is evidenced by measuring the coherence ρ_{35}, the relevant "yield" shown in the right y-axis of (a). The calculation was performed with $H = A\vec{I}\cdot\vec{s}_D + B(s_{Dz} + s_{Az})$, $k_S = k_T = A/20$, $\gamma =$ A/2000 and initial state $|S\rangle \otimes |\uparrow\rangle$.

We will now demonstrate the utility of I_{ex}. A central observable in RP reactions is the magnetic field effect [33], i.e. the reaction yield dependence on the applied magnetic field B. For example, considering the singlet reaction yield $Y_S = \int dr_S$, the dependence $Y_S(B)$, the dependence stems from the modulation of the S-T mixing by the Zeeman terms $B(s_{Dz} + s_{Az})$ of the donor and acceptor electron entering the Hamiltonian.

In Fig.3.3.(a) we plot (left y-axis) the ordinary field effect $Y_S(B)$, depicting the low-field effect due to zero-field level crossings, and the high-field effect due to the triplet states shifting out of resonance with the singlet [34]. In Fig.3.3.(b) we plot the $B-$dependence of the integrated extracted information,$I_{ex}(B)$. Apparently, the quantity also conveys the low-field and the high-field effect. Interestingly though, it carries additional information, as evidenced by the dip at $B = A$. The reason that this new field-effect is not observed in the singlet reaction yield of Fig.3.3.(b) is that measuring the singlet character of the RP state is not optimal for extracting this particular field effect. By changing the measurement, and instead of the projector Q_S, measuring the absolute value of the element ρ_{35} of the density matrix we can observe such a field effect, as seen in Fig.3.3.(a) (right y-axis). This matrix element corresponds to the coherence $|\uparrow\downarrow\rangle\langle\downarrow\uparrow| \otimes |\Uparrow\rangle\langle\Uparrow|$.

The new field effect is due to level-crossings that appear when expressing the density matrix ρ and its non-reacting evolution law in Liouville space. This will be explored in detail elsewhere, together with the discussion on how to perform generalized measurements optimally extracting the information that can in principle be extracted, by $I_{ex}(B)$. To explain in detail the low and high magnetic field effects we show in the table 3.1 the eigenvalues and the eigenstates of the Hamiltonian used in the simulations and we plot in Figure 3.5 the eigenvalues as a function of the magnetic field. We also plot in Figure 3.4 the energies of the singlet and triplet states as a function of the magnetic field's magnitude. The idea of the low field effect as described in [33] is that in zero magnetic field we have as you can see in figure[3.5] degeneracy of the energy levels.When we increase a little bit the magnetic field the degeneracy is lifted, thus there are more ways of singlet-triplet mixing as you can also see from the table, thus the radical pair stays for longer time in triplet state.This is the reason we see a reduction in the singlet yield.This can also be seen from the figure 3.4 where in low magnetic fields all triplet states are energetically close to singlet and thus they can be easily mixed. In a more mathematical way, if we write the density matrix in the basis of the zero field eigenstates, we can see some off-diagonal matrix elements know as the zero quantum coherences. Zero quantum coherences are responsible for the singlet-triplet mixing in the zero field regime. When we apply a weak magnetic field the coherences are increased, thus there are more channels available for singlet-triplet mixing. In the high field regime, there is only mixing between the states $S - T_0$ hence, there is again an increase in the yield.

Eigenstates	Eigenvalues
$\vert\psi_1\rangle = \frac{1}{\sqrt{2}}(\vert\mathrm{T}_0,\uparrow\rangle - \vert S,\uparrow\rangle)$	$\mathrm{E}_1 = \frac{A}{4}$
$\vert\psi_2\rangle = \frac{1}{\sqrt{2}}(\vert S,\uparrow\rangle + \vert T_0,\uparrow\rangle)$	$\mathrm{E}_2 = \frac{A}{4}$
$\vert\psi_3\rangle = \vert T_+,\uparrow\rangle$	$\mathrm{E}_3 = \frac{1}{4}(A - 4B)$
$\vert\psi_4\rangle = \vert T_-,\downarrow\rangle$	$\mathrm{E}_4 = \frac{1}{4}(A + 4B)$
$\vert\psi_5\rangle = c_1\vert T_+,\downarrow\rangle + \frac{c_2}{\sqrt{2}}(\vert S,\uparrow\rangle + \vert T_0,\uparrow\rangle)$	$\mathrm{E}_5 = \frac{1}{4}(-A - 2B - 2\sqrt{A^2 + B^2})$
$\vert\psi_6\rangle = c_2\vert T_-,\uparrow\rangle + \frac{c_1}{\sqrt{2}}(\vert T_0,\downarrow\rangle - \vert S,\downarrow\rangle)$	$\mathrm{E}_6 = \frac{1}{4}(-A + 2B - 2\sqrt{A^2 + B^2})$
$\vert\psi_7\rangle = c_3\vert T_+,\downarrow\rangle + \frac{c_4}{\sqrt{2}}(\vert T_0,\uparrow\rangle + \vert S,\uparrow\rangle)$	$\mathrm{E}_7 = \frac{1}{4}(-A - 2B + 2\sqrt{A^2 + B^2})$
$\vert\psi_8\rangle = c_4\vert T_-,\uparrow\rangle + \frac{c_3}{\sqrt{2}}(\vert T_0,\downarrow\rangle - \vert S,\downarrow\rangle)$	$\mathrm{E}_8 = \frac{1}{4}(-A + 2B + 2\sqrt{A^2 + B^2})$

TABLE 3.1: Eigenstates and eigenvalues of the Hamiltonian $H = A\vec{I} \cdot \vec{s}_D + B(s_{Dz} + s_{Az})$

where:

$$c_1 = \frac{-B - \sqrt{A^2 + B^2}}{\sqrt{A^2 + (B + \sqrt{A^2 + B^2})^2}} \tag{3.19}$$

$$c_2 = \frac{A}{\sqrt{A^2 + (B + \sqrt{A^2 + B^2})^2}} \tag{3.20}$$

$$c_3 = \frac{-B + \sqrt{A^2 + B^2}}{\sqrt{A^2(-B + \sqrt{A^2 + B^2})^2}} \tag{3.21}$$

$$c_4 = \frac{A}{\sqrt{A^2(-B + \sqrt{A^2 + B^2})^2}} \tag{3.22}$$

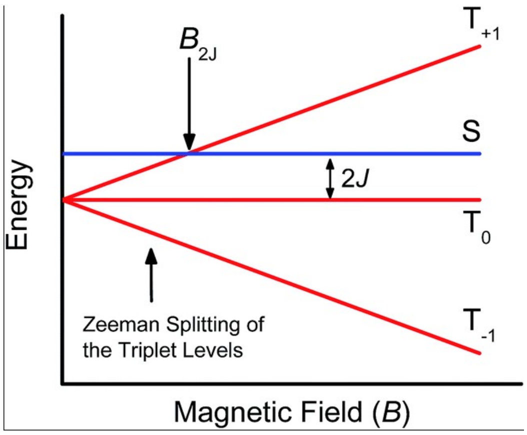

FIGURE 3.4: Singlet and triplet energy states as a function of the magnetic field's magnitude. $2J$ is the energy difference between the states $S - T_0$ and it is a function of the distance between the two interactiong spins $J(r) = J_0 e^{-r/r_0}$.

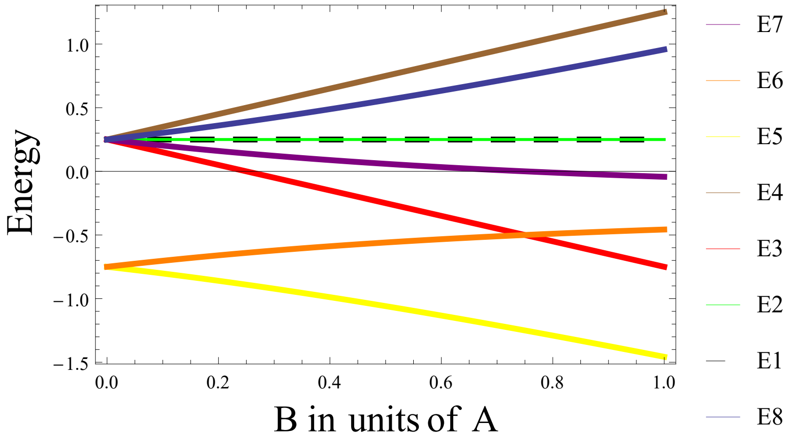

FIGURE 3.5: Eigenstates of the Hamiltonian $H = A\vec{I} \cdot \vec{s}_D + B(s_{Dz} + s_{Az})$, as a function of the magnetic field's magnitude when $A = 1$.

Magnetic field effects in the radical pair mechanism have been studied extensively and except from theory there are also some remarkable experiments in the field. A relatively recent experiment on radical pairs [37] showed a high sensitivity of the absorption in the magnitude and direction of the magnetic field. They used an experimental configuration of two pairs of Helmholtz coils in order to create a large area of homogeneous magnetic field in the middle. They used carotenoid-porphyrin-fullerene radical pairs $[C^{\bullet +} - P - F^{\bullet -}]$ for the measurements where a pulsed probe laser at 532nm with power 5 mJ generates the reaction and a pump laser was used for the absorption. The important results are depicted in the following plots. As you can see, there is a dependence of the absorption on the magnitude of the magnetic field. The blue results differ from the red in the delay time after the activation of the reaction. Each dot in the plot indicates a measurement and sequential measurement differ by 50ns.

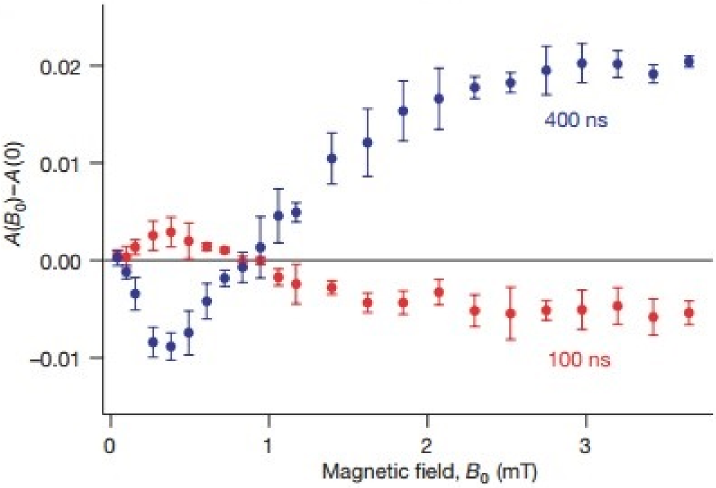

FIGURE 3.6: Changes in the transient absorption $A(B_0)-A(0)$ of $[C^{\bullet+}-P-F^{\bullet-}]$ at $119K$ averaged over a 50ns period centered at 100ns and 400ns after its formation. Maeda et.al., Nature , 453, 387-390 (15 May 2008)

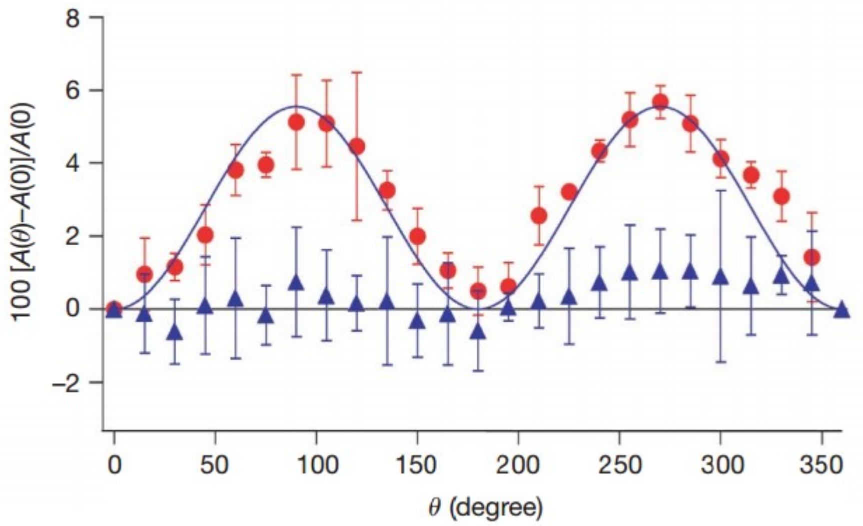

FIGURE 3.7: The red dots show the dependence of the $[C^{\bullet+}-P-F^{\bullet-}]$ absorption on the direction of the magnetic field θ. The solid line is the best fit to a $sin^2\theta$ form. The blue dots are the signals detected when the polarization axis of the probe light was z (that is, vertical). No θ-dependence is expected or seen.Errors bars, ±1 s.d., Maeda et.al., Nature , 453, 387-390 (15 May 2008)

3.4 Conclusions-Discussion

In summary, we introduced the quantum information and entropy perspective in radical-pair reactions, which are a central paradigm in the new field of quantum biology. This approach serves as a testbed for our understanding of the fundamental quantum dynamics of the radical-pair mechanism, ruling out the master equation traditionally used until now. For example, considering the entropy of radical-pairs along the lines of [28] is not even possible in the first place, since the density matrices introduced in [28] in the attempt to consistently describe radical-pair quantum trajectories from Haberkorn's perspective have negative eigenvalues[29]. Finally, our approach also leads to a deeper insight of the metrological aspect of these reactions, which realize a quantum magnetometer in a biochemical context, revealing magnetic field effects conveyed by the information extracted during the reaction.

Bibliography

[1] S. F. Huelga and M. B. Plenio, *Vibrations, quanta and biology,*. Contemp. Phys. 54, 181 (2013).

[2] M. Mohseni, Y. Omar, G. S. Engel and M. B. Plenio, *Quantum effects in biology* Cambridge University Press,Cambridge, 2014).

[3] I. K. Kominis, *The radical-pair mechanism as a paradigm for the emerging science of quantum biology,* Mod. Phys.Lett. B 29, 1530013 (2015).

[4] G. D. Scholes, G.R. Fleming, A. Olaya-Castro and R. van Grondelle, *Lessons from nature about solar light harvesting,*. Nat. Chem. 3, 763 (2011).

[5] G. S. Engel et al., *Evidence for wavelike energy transfer through quantum coherence in photosynthetic systems,*. Nature 446, 782 (2007).

[6] G. Panitchayangkoon et al., *Long-lived quantum coherence in photosynthetic complexes at physiological temperature,*. Proc. Natl. Acad. Sci. U.S.A. 107, 12766 (2010).

[7] E. Collini et al., *Coherently wired light-harvesting in photosynthetic marine algae at ambient temperature,*. Nature 463, 644 (2010).

[8] M. Mohseni, P. Rebentrost, S. Lloyd and A. Aspuru Guzik, *Environment-Assisted Quantum Walks in Energy Transfer of Photosynthetic Complexes,*. J. Chem. Phys. 129, 1 (2008).

[9] R. Caruso, A. W. Chin, A. Datta, S. F. Huelga and M. B. Plenio, *Highly efficient energy excitation transfer in light-harvesting complexes: the fundamental role of noise-assisted transport,*. J. Chem. Phys. 131, 105106 (2009).

[10] I. K. Kominis, *Quantum Zeno effect explains magnetic sensitive radical-ion-pair reactions,*. Phys. Rev. E 80, 056115 (2009).

[11] I. K. Kominis, *Radical-ion-pair reactions are the biochemical equivalent of the optical double slit experiment,*. Phys.Rev. E 83, 056118 (2011).

[12] M. Kritsotakis and I. K. Kominis, *Retrodictive derivation of the radical-ion-pair master equation and Monte Carlo simulation with single-molecule quantum trajectories,*. Phys. Rev. E 90, 042719 (2014).

[13] K. M. Vitalis and I. K. Kominis, *Lamb shift in radical-ion pairs produces a singlet-triplet energy splitting in photosynthetic reaction centers,*. Eur. Phys. J. Plus 129, 187 (2014).

[14] K. Tsampourakis and I. K. Kominis, *Quantum trajectory tests of radical-pair quantum dynamics in CIDNP measurements of photosynthetic reaction centers,*. Chem.Phys. Lett. 640, 40 (2015).

[15] C. Y. Cai, Qing Ai, H. T. Quan and C. P. Sun, *Sensitive chemical compass assisted by quantum criticality,*. Phys.Rev. A 85, 022315 (2012).

[16] J. Cai and M. B. Plenio, *Chemical Compass Model for Avian Magnetoreception as a Quantum Coherent Device,*. Phys. Rev. Lett. 111, 230503 (2013).

[17] B.-M. Xu, J. Zou, J.-G. Li, and B. Shao, *Estimating the hyperfine coupling parameters of the avian compass by comprehensively considering the available experimental results,*. Phys. Rev. E 88, 032703 (2013).

[18] J. A. Pauls, Y. Zhang, G. P. Berman, and S. Kais, *Quantum coherence and entanglement in the avian compass,*. Phys. Rev. E 87, 062704 (2013).

[19] K. Schulten, *Magnetic field effects in chemistry and biology,*. Adv. Solid State Phys. 22, 61 (1982).

[20] T. Ritz, S. Adem and K. Schulten, *A model for photoreceptor-based magnetoreception in birds,*. Biophys.J. 78, 707 (2000).

[21] W. Wiltschko and R. Wiltscko, *Magnetic orientation and magnetoreception in birds and other animals,*. J. Comp.Physiol. A 191, 675 (2005).

[22] I. F. Cespedes-Camacho and J. Matysik, *in The biophysics of photosynthesis, Eds. J. Goldbeck and A. van der Est*. (Springer Science + Business Media, New York, 2014)

[23] U. Steiner and T. Ulrich, *Magnetic field effects in chemical kinetics and related phenomena,*. Chem. Rev. 89, 51 (1989).

[24] R. Haberkorn, *Density matrix description of spin-selective radical pair reactions,*. Mol. Phys. 32, 1491 (1976).

[25] M. Ozawa, *On information gain by quantum measurements of continuous observables,*. J. Math. Phys. 27, 759 (1986).

[26] O. E. Lanford and D. Robinson, *Mean entropy of states in quantum-statistical mechanics,*. J. Math.Phys. 9, 1120 (1968).

[27] K. Jacobs, *Quantum measurement theory and its applications* . (Cambridge University Press, Cambridge, 2014).

[28] G. Jeschke, *Comment on "Quantum trajectory tests of radical-pair quantum dynamics in CIDNP measurements of photosynthetic reaction centers",*. Chem. Phys. Lett. 648, 200 (2016).

[29] I. K. Kominis, *Reply to the comment on "Quantum trajectory tests of radical-pair quantum dynamics in CIDNP measurements of photosynthetic reaction centers" by G.Jeschke,*. Chem. Phys. Lett. 648, 204 (2016).

[30] T. Baumgratz, M. Cramer and M. B. Plenio, *Quantifying Coherence,*. Phys. Rev. Lett. 113, 140401 (2014).

[31] H.-P. Breuer, E.-M. Laine, J. Piilo and B. Vacchini, *Colloquium: Non-Markovian dynamics in open quantum systems,*. Rev. Mod. Phys. 88, 021002 (2016).

[32] *The 8 basis kets are* $|S\rangle \otimes |\uparrow\rangle , |S\rangle \otimes |\downarrow\rangle , |T_+\rangle \otimes |\uparrow\rangle , |T_+\rangle \otimes |\downarrow\rangle , |T_-\rangle \otimes |\uparrow\rangle , |T_-\rangle \otimes |\downarrow\rangle , |T_0\rangle \otimes |\uparrow\rangle , |T_0\rangle \otimes |\downarrow\rangle$. *The two-electron state is on the left of the tensor product and the nuclear spin state on the right. The former is spanned by the singlet* $|S\rangle = \frac{1}{\sqrt{2}}(|\uparrow\downarrow\rangle - |\downarrow\uparrow\rangle)$ *and the triplets* $|T_0\rangle = \frac{1}{\sqrt{2}}(|\uparrow\downarrow\rangle + |\downarrow\uparrow\rangle), |T_+\rangle = |\uparrow\uparrow\rangle , |T_-\rangle = |\downarrow\downarrow\rangle$. *Although obvious, we mention that the RP model we choose (i.e. one nuclear spin instead of several, and the particular Hamiltonian chosen) is of no concern, since we here demonstrate a violation of a fundamental law of entropy by the foundational theory of spin chemistry. As well known, it takes infinite examples to establish a theory, but only one and any counter-example to invalidate it.*

[33] C. T. Rodgers, *Magnetic field effects in chemical systems,*. Pure Appl. Chem. 81, 19 (2009).

[34] C. R. Timmel et al., *Effects of weak magnetic fields on free radical recombination reactions,*. Mol. Phys. 95, 71 (1998).

[35] S. L. Braunstein and C. M. Caves, *Statistical distance and the geometry of quantum states,*. Phys. Rev. Lett. 72, 3439 (1994).

[36] M.Tiersch and H.J.Briegel, *Decoherence in the chemical compass:the role of decoherence for avian magnetoreception,*. Phil.Trans.R.Soc.A 2012 ,370,4517-4540

[37] Maeda et.al., *Chemical compass model of avian magnetoreception*. Nature , 453, 387-390 (2008)

[38] K.Mouloudakis and I.K.Kominis, *Revealing the properties of the radical-pair magnetoreceptor using pulsed photo-excitation timed with pulsed rf.* Biosystems 147, 35 (2016)

[39] K.Mouloudakis and I.K.Kominis, *Quantum Information Processing in the Radical-Pair Mechanism*. arXiv:1607.03071